



**HAL**  
open science

## On the optimal experimental design for heat and moisture parameter estimation

Julien Berger, Denys Dutykh, Nathan Mendes

► **To cite this version:**

Julien Berger, Denys Dutykh, Nathan Mendes. On the optimal experimental design for heat and moisture parameter estimation. 2016. hal-01334414v1

**HAL Id: hal-01334414**

**<https://hal.science/hal-01334414v1>**

Preprint submitted on 20 Jun 2016 (v1), last revised 11 Oct 2016 (v2)

**HAL** is a multi-disciplinary open access archive for the deposit and dissemination of scientific research documents, whether they are published or not. The documents may come from teaching and research institutions in France or abroad, or from public or private research centers.

L'archive ouverte pluridisciplinaire **HAL**, est destinée au dépôt et à la diffusion de documents scientifiques de niveau recherche, publiés ou non, émanant des établissements d'enseignement et de recherche français ou étrangers, des laboratoires publics ou privés.



Distributed under a Creative Commons Attribution - NonCommercial - ShareAlike 4.0 International License

Julien BERGER

*Pontifical Catholic University of Paraná, Brazil*

Denys DUTYKH

*CNRS-LAMA, Université Savoie Mont Blanc, France*

Nathan MENDES

*Pontifical Catholic University of Paraná, Brazil*

ON THE OPTIMAL EXPERIMENTAL  
DESIGN FOR HEAT AND MOISTURE  
PARAMETER ESTIMATION

LAST MODIFIED: June 20, 2016

# ON THE OPTIMAL EXPERIMENTAL DESIGN FOR HEAT AND MOISTURE PARAMETER ESTIMATION

JULIEN BERGER\*, DENYS DUTYKH, AND NATHAN MENDES

**ABSTRACT.** In the context of estimating material properties of porous walls based on in-site measurements and identification method, this paper presents the concept of Optimal Experiment Design (OED). It aims at searching the best experimental conditions in terms of quantity and position of sensors and boundary conditions imposed to the material. These optimal conditions ensure to provide the maximum accuracy of the identification method and thus the estimated parameters. The search of the OED is done using the FISHER information matrix and a priori knowledge on the parameters. The methodology is applied for two cases. The first one deals with purely conductive heat transfer, while the second one combines a strong coupling between heat and moisture transfer.

**Key words and phrases:** inverse problem; parameter estimation; Optimal Experiment Design (OED); heat and moisture transfer; sensitivity functions

**MSC:** [2010] 35R30 (primary), 35K05, 80A20, 65M32 (secondary)

**PACS:** [2010] 44.05.+e (primary), 44.10.+i, 02.60.Cb, 02.70.Bf (secondary)

---

*Key words and phrases.* inverse problem; parameter estimation; Optimal Experiment Design (OED); heat and moisture transfer; sensitivity functions.

\* Corresponding author.

## 1. Introduction

Heating or cooling strategies for buildings are commonly based on numerical models considering the physical phenomena occurring, which can be calibrated using on-site measurements for estimating the properties of the materials constituting the walls in order to reduce the discrepancies between model predictions and real performance.

Several experimental works at the scale of the wall can be reported from the literature. Instrumented test cells, as ones presented in [5–8, 11, 16, 19, 20] provide measured dataset as temperature and relative humidity at different points in the wall for given boundary conditions. Some experiments at the scale of the whole-building are described in [4, 10]. These data can be used to estimate the properties (transport and capacity coefficients) of the materials as reported for instance in [13, 22] for heat transfer and in [17, 24] for coupled heat and moisture transfer.

The estimation of the material properties based on measurements and identification methods is illustrated in Figure 1. For a given model, the experimental design defines the inputs (boundary and initial conditions) and the type of sensors as well as their quantity and location. From a measured field (generally called the observation), identification methods are used to estimate the unknown parameters  $\mathbf{P}$  of the model, *i.e.* the wall thermo-physical properties.

The accuracy of the solution strongly depends on the experiment design. The choice of the measurement devices and the inputs have consequences on the accuracy of the parameter estimated. Furthermore, due to the correlation between the parameters, multiple local solutions of the estimation problem exist. Hence, one can address the following questions: what are the best experimental conditions to provide the best conditioning of the identification method? In particular, how many sensors are necessary? Where are their best location? What boundary and initial conditions should be imposed? Can we really choose them?

These issues deal with searching the Optimal Experiment Design (OED) that enables to identify the parameters  $\mathbf{P}$  of a model with a maximum precision. A first objective of the OED is to adjust the inputs in order to maximize the sensitivity of the output field  $u$  to parameters  $\mathbf{P}$ . A second objective is to find the optimum location and quantity of sensors. The achievement of these objectives enables to determine conditions of the experiments under which the identification of the parameters will have the maximum accuracy.

The search of the OED is based on quantifying the amount of information contained by the observed field  $u_{\text{exp}}$ . For this, FISHER information matrix is used [9, 23], considering both the model sensitivity, the measurement devices and the parameter correlation. The sensitivity of the output field  $u$  with respect to the model parameters  $\mathbf{P}$  is calculated, corresponding to the sensitivity of the cost function of the parameter estimation problem. The higher the sensitivity is, the more information is available in the measurement data and the more accurate is the identification of the parameters. Generally speaking, the methodology of searching the OED is important before starting any experiments aiming at

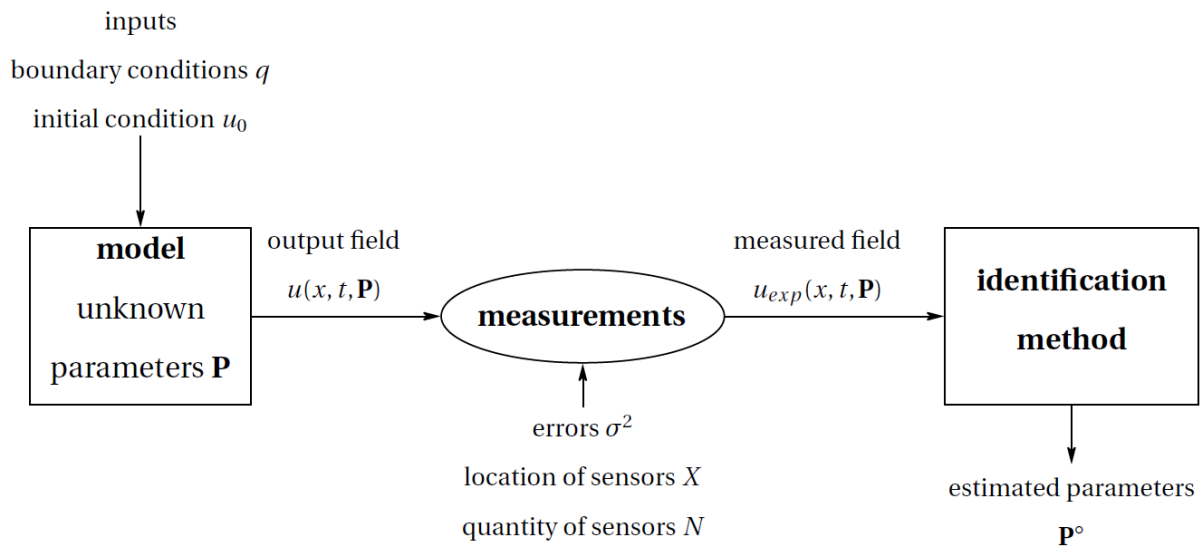


**Figure 1.** *Parameter estimation process.*

solving estimation parameter problems. It allows choosing with a deterministic approach the conditions of the experiments. Furthermore, it provides informations on the accuracy of the solution of the estimation problems.

Several works can be reported on the investigation of the OED. In [1], the OED is planned as a function of the quantity of sensors and their location, for the estimation of boundary heat flux of non-linear heat transfer. In [9], the OED is searched for the estimation of transport coefficient in convection-diffusion equation. In [14], the OED is analysed as a function of the boundary heat flux for the identification of the radiative properties of the material. In [12], the OED is investigated for thermal dispersion coefficients in porous media as a function of the positions of the sensors. However, the application of OED theory for non-linear heat and moisture transfer with application for the estimation of the properties of a wall is relatively rare.

This article presents the methodology of searching the OED for experiments aiming at solving estimation parameter problems. In the first section, the concept of OED is detailed for an inverse problem of non-linear heat transfer. The computation of the model sensitivity to the parameter is specified. The OED is sought as a function of the quantity and location of sensors as well as the amplitude and the frequency of the heat flux at the material boundaries. Then the OED for the estimation of hygrothermal properties considering non-linear heat and moisture transfer is investigated. Finally, some main conclusions and perspectives are outlined in the last Section.

## 2. Optimal experiment design for non-linear heat transfer problem

First, the methodology of searching the OED is detailed for an inverse problem of non-linear heat transfer. A brief numerical example is given to illustrate the results.

### 2.1. Physical problem and mathematical formulation

The physical problem considers an experiment involving a multi-dimensional transient heat conduction problem in domains  $x \in \Omega = [0, 1]$  and  $t \in [0, \tau]$ . The initial temperature in the body is supposed uniform. The surface of the boundary  $\Gamma_D = \{x = 1\}$  is maintained at the temperature  $u_D$ . A time-harmonic heat flux  $q$ , of amplitude  $A$  and frequency  $\omega$ , is imposed at the surface of the body denoted by  $\Gamma_q \{x = 0\}$ . Therefore, the mathematical formulation of the heat conduction problem can be written as:

$$c^* \frac{\partial u}{\partial t^*} - \frac{\partial}{\partial x^*} \left( k^*(u) \frac{\partial u}{\partial x^*} \right) = 0, \quad x^* \in \Omega, t^* \in ]0, \tau], \quad (2.1a)$$

$$u = u_D \quad x^* \in \Gamma_D, t > 0, \quad (2.1b)$$

$$k^*(u) \frac{\partial u}{\partial x^*} = A^* \sin(2\pi\omega^*t^*) \quad x^* \in \Gamma_q, t > 0, \quad (2.1c)$$

$$u = u_0(x^*) \quad x^* \in \Omega, t^* = 0, \quad (2.1d)$$

$$k^*(u) = (k_0^* + k_1^*u) \quad (2.1e)$$

where the following dimensionless quantities are introduced:

$$x^* = \frac{x}{L}, \quad u = \frac{T}{T_{ref}}, \quad u_D = \frac{T_D}{T_{ref}}, \quad u_0 = \frac{T_0}{T_{ref}}, \quad k_0^* = \frac{k_0}{k_r},$$

$$k_1^* = \frac{k_1 T_{ref}}{k_{ref}}, \quad c^* = \frac{c}{c_{ref}}, \quad t_{ref} = \frac{c_{ref} L^2}{k_{ref}}, \quad A^* = \frac{AL}{k_{ref} T_{ref}}, \quad \omega^* = \omega t_{ref}$$

where  $T$  is the temperature,  $c$  the volumetric heat capacity,  $k_0$  the thermal conductivity and  $k_1$  its dependency on temperature,  $L$  the linear dimension of the material,  $A$  the intensity and  $\omega$  the frequency of the flux imposed on surface  $\Gamma_q$ . Subscripts *ref* accounts for a characteristic reference value, *D* for the DIRICHLET boundary conditions, zero (0) for the initial condition of the problem and superscript  $\star$  for dimensionless parameters.

The problem given by Eqs. (2.1)(a-e) is a direct problem when all the thermo-physical properties, initial and boundary conditions, as well as the body geometry are known. Here, we focus on the inverse problem consisting in estimating one or more parameters of the material properties (as  $c$ ,  $k_0$  and/or  $k_1$ ) using the mathematical model Eqs. (2.1)(a-e) and a measured temperature data  $u_{exp}$  obtained by  $N$  sensors placed in the material at  $\mathbf{X} = [x_n], n \in \{1, \dots, N\}$ . The  $M$  unknown parameters are here denoted as vector

$\mathbf{P} = [p_m]$ ,  $m \in \{1, \dots, M\}$ . The solution of the inverse problem is done by the minimisation of the cost function:

$$J[\mathbf{P}] = \|u_{\text{exp}} - \mathfrak{T}(u(x, t, \mathbf{P}))\|^2 \quad (2.2)$$

where  $u$  is the solution of the transient heat conduction problem Eqs. (2.1)(a-e).  $u_{\text{exp}}$  are the data obtained by experiments. They are obtained by  $N$  sensors providing a time discrete measure of the field at specified points within the material.  $\mathfrak{T}$  is the operator allowing to compare the solution  $u$  at the same space-time points where observations  $u_{\text{exp}}$  are taken.

Several inverse problems can be associated to Eqs. (2.1)(a-e). One aims at estimating one parameter:  $m = 1$  and  $\mathbf{P} = c$ ,  $\mathbf{P} = k_0$  or  $\mathbf{P} = k_1$ . Others aim at estimating a group of  $m = 2$  or  $m = 3$  parameters. In this work, the optimal experiment design will be investigated for both cases.

## 2.2. Optimal experiment design

Efficient computational algorithms for recovering parameters  $\mathbf{P}$  have already been proposed. Readers may refer to [15] for a primary overview of different methods. They are based on the minimisation of the cost function  $J[\mathbf{P}]$ . For this, it is required to equate to zero the derivatives of  $J[\mathbf{P}]$  with respect to each of the unknown parameters  $p_m$ . Such necessary condition for the minimisation of  $J[\mathbf{P}]$  can be represented by the sensitivity function as:

$$\Theta_m(x, t) = \frac{\partial J}{\partial p_m} = \frac{\partial u}{\partial p_m}, \quad \forall m \in \{1, \dots, M\} \quad (2.3)$$

The sensitivity function  $\Theta_m$  measures the sensitivity of the estimated field  $u$  with respect to change in the parameter  $p_m$  [1, 14, 15]. A small value of the magnitude of  $\Theta_m$  indicates that large changes in  $p_m$  yield small changes in  $u$ . The estimation of parameter  $p_m$  is therefore difficult in such case. When the sensitivity coefficient  $\Theta_m$  is small, the inverse problem is ill-conditioned. If the sensitivity coefficients are linearly dependent, the inverse problem is also ill-conditioned. Therefore, to get an optimal evaluation of parameters  $\mathbf{P}$ , it is desirable to have linearly-independent sensitivity functions  $\Theta_m$  with large magnitude for all parameters  $p_m$ . These conditions ensure the best conditioning of the computational algorithm to solve the inverse problem and thus the better accuracy of the estimated parameter.

It is possible to define the experimental design in order to reach these conditions. The issue is to find the optimal quantity of sensors  $N^\circ$ , their optimal location  $\mathbf{X}^\circ$ , the optimal amplitude  $A^\circ$  and the optimal frequency  $\omega^\circ$  of the flux imposed at the surface  $\Gamma_q$ . To search this optimal experiment design, we introduce the following measurement plan:

$$\pi = \{N, \mathbf{X}, A, \omega\} \quad (2.4)$$



In analysis of optimal experiment for inverse problems, a quality index describing the accuracy of recovering the unknown parameter  $\mathbf{P}$  is the  $D$ -optimum criterion [1, 2, 9, 14, 23]:

$$\Psi = \det [F(\pi)] \quad (2.5)$$

where  $F(\pi)$  is the normalized FISHER information matrix [9, 23]:

$$F(\pi) = \frac{1}{N} [\Phi_{ij}], \quad \forall (i, j) \in \{1, \dots, M\}^2 \quad (2.6a)$$

$$\Phi_{ij} = \sum_{n=1}^N \int_0^\tau \sigma^2 \Theta_i(x_n, t) \Theta_j(x_n, t) dt \quad (2.6b)$$

where  $\sigma$  is the variance of the error of measuring  $u_{\text{exp}}$ , considered in this work as a constant equal for all the measurement points.

The matrix  $F(\pi)$  characterises the total sensitivity of the system as a function of measurement plan  $\pi$  Eqs. (2.4). The search of the OED aims at finding a measurement plan  $\pi^*$  for which the objective function Eq. (2.5) reaches the maximum value:

$$\pi^\circ = \{N^\circ, \mathbf{X}^\circ, A^\circ, \omega^\circ\} = \arg \max_{\pi} \Psi \quad (2.7)$$

The solution of this problem is built by successive iterations done on the measurement plan  $\pi$ :

**Step 1.** For a fixed value of the measurement plan  $\pi = \{N, \mathbf{X}, A, \omega\}$ , the direct problem defined by Eqs. (2.1)(a-e) is computed. In this work, it is solved by using a finite-difference standard discretizations. An embedded adaptive in time RUNGE-KUTTA scheme combined with central spatial discretization is used. It is adaptive and embedded to estimate local error with little extra cost.

Given the solution  $u$  of the direct problem 2.1(a-e) for a fixed value of the measurement plan, the next step consists in computing  $\Theta_m = \frac{\partial u}{\partial p_m}$  by solving the sensitivity problem associated to parameter  $p_m$ :

$$c \frac{\partial \Theta_m}{\partial t} - \frac{\partial}{\partial x} \left( k \frac{\partial}{\partial x} \Theta_m \right) = - \frac{\partial c}{\partial p_m} \frac{\partial u}{\partial t} + \frac{\partial u}{\partial x} \frac{\partial}{\partial p_m} \left( \frac{\partial k}{\partial x} \right) + \frac{\partial k}{\partial p_m} \frac{\partial^2 u}{\partial x^2} \quad x \in \Omega, t > 0, \quad (2.8a)$$

$$\Theta_m = 0 \quad x \in \Gamma_d, t > 0, \quad (2.8b)$$

$$k \frac{\partial \Theta_m}{\partial x} = \frac{\partial u}{\partial x} \frac{\partial k}{\partial p_m} \quad x \in \Gamma_q, t > 0, \quad (2.8c)$$

$$\Theta_m = 0 \quad x \in \Omega, t = 0, \quad (2.8d)$$

$$k = (k_0 + k_1 u) \quad (2.8e)$$

The sensitivity problem Eqs. (2.8) is also solved using an embedded adaptive in time RUNGE-KUTTA scheme combined with central spatial discretization. It is important to

note that the resolution of the sensitivity problem (2.8)(a-e) requires *a priori* knowledge about the unknown parameters  $\mathbf{P}$ .

**Step 2.** The FISHER matrix (2.6)(a,b) and the  $D$ -optimum criterion (2.5) are calculated. The iterations continue to Step 1, for other fixed values of the measurement plan  $\pi$ .

## 2.3. Numerical example

Current section illustrates the search of optimum experiment design for problem Eqs. (2.1) considering  $u_0 = u_D = 1$ . The dimension less properties of the material are equal to  $c^* = 10.9$ ,  $k_0^* = 1$ ,  $k_1^* = 0.12$ . The final simulation time of the experiment is fixed to  $\tau = 28.3$ .

From a physical point of view, the numerical values correspond to a material of length  $L_r = 0.1$  m. The thermal properties were chosen from a the wood fibre:  $c = 3.92 \cdot 10^5$  J/m<sup>3</sup>/K,  $k_0 = 0.118$  W/m/K and  $k_1 = 5 \cdot 10^{-4}$  W/m/K<sup>2</sup>. The initial temperature of the material is considered uniform at  $T_0 = T_{ref} = 293.15$  K. The temperature at the boundary  $\Gamma_D$  is maintained at  $T_D = T_{ref} = 293.15$  K. The characteristic time of the problem is  $t_{ref} = 3050$  s. Thus, the total time of the experiments corresponds to 24h. A schematic view of the problem is given in Figure 2(a).

As mentioned in previous section, the OED is sought as a function of the quantity of sensors  $N$ , their location  $\mathbf{X}$ , the amplitude  $A$  and frequency  $\omega$  of the flux imposed at the surface  $\Gamma_q$ . For the current numerical application, we consider a maximum of  $N = 4$  possible sensors. Their location varies from  $\mathbf{X} = [0]$  for  $N = 1$  and  $\mathbf{X} = [0 \ 0.25 \ 0.5 \ 0.75]$  for  $N = 4$  as shown in Figure 2(a). For the amplitude  $A$ , 5 values are considered in the interval  $[0.2, 1]$  with a regular mesh of 0.2. The minimal value of  $A$  corresponds to a physical heat flux of 70 W/m<sup>2</sup>. For the frequency, 30 values have been taken in the interval  $[10^{-3}, 1]$ . The extreme values of the heat flux are illustrated in Figure 2(b).

### 2.3.1 Estimation of one single parameter

Considering previous description of the numerical example, we first focus on the search of the OED for solving an inverse problem (IP) for one parameter. Thus  $\mathbf{P}$  equals to  $c$ ,  $k_0$  or  $k_1$ . Figures 3(a-c) show the variation of the criterion  $\Psi$  as a function of the amplitude  $A$  and the frequency  $\omega$  of the heat flux. For each of the inverse problems, the criterion is maximum for a low frequency and for a large amplitude as presented in Figure 6. Numerical values of the OED  $\pi^\circ$  are given in Table 1. In terms of physical numerical values, the OED is reached for a heat flux of amplitude 350 W/m<sup>2</sup> and a period of 17.3 h, 60.6 h and 53.5 h for estimating parameter  $c$ ,  $k_0$  or  $k_1$ , respectively.

The effect of the numbers of sensors and their positions is given in Figures 4(a-c) for a fixed amplitude. Adding new sensors is not necessary to recover one parameter ( $c$ ,  $k_0$  or  $k_1$ ). One sensor is sufficient to get an OED. It can be noticed that the optimal parameter  $\omega^\circ$  does not vary with the quantity of sensors. This sensor has to be located on the boundary

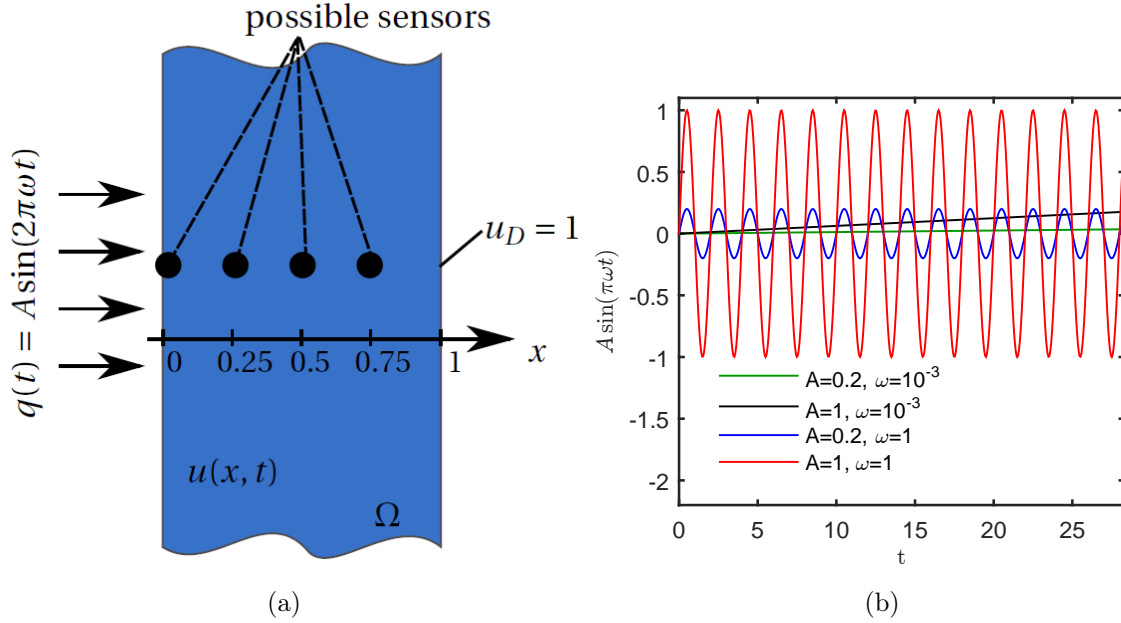


**Figure 2.** Schematic view of experimental design (a) and the extreme values of the heat flux (b).

receiving the heat flux. Indeed, the boundary  $\Gamma_q$  is where the sensitivity coefficient of the parameter has the largest magnitude as shown in Figures 5(a-c) correspondingly.

### 2.3.2 Estimation of several parameters

Now we focus on a single experiment design for estimating all 3 parameters  $\mathbf{P} = (c, k_0, k_1)$  simultaneously. Figure 3(d) gives the variation of the criterion  $\Psi$  as a function of the amplitude  $A$  and the frequency  $\omega$  of the heat flux. The optimum experiment design is reached for a low frequency and a large amplitude as reported in Table 1. A heat flux with a sinusoidal period of 25.2 h provides the OED. Figure 3(d) shows the variation of the criterion  $\Psi$  as a function of the quantity of sensors and their location. A single sensor located on the surface  $\Gamma_q \equiv \{x = 0\}$  where the sensitivity coefficients of the parameters have the largest amplitude. It can be noticed in Figure 3(d) that the sensitivity coefficients are linearly-independent. It provides a good conditioning of the computational algorithm for solving the inverse problem of parameters  $\mathbf{P} = (c, k_0, k_1)$ . Nevertheless, it can be noted that the sensitivity of parameter  $k_1$  has a low magnitude. The solution of the inverse problem might not give an accurate estimation for this parameter. To deal with this issue, the amplitude  $A^\circ$  of the heat flux can be increased.

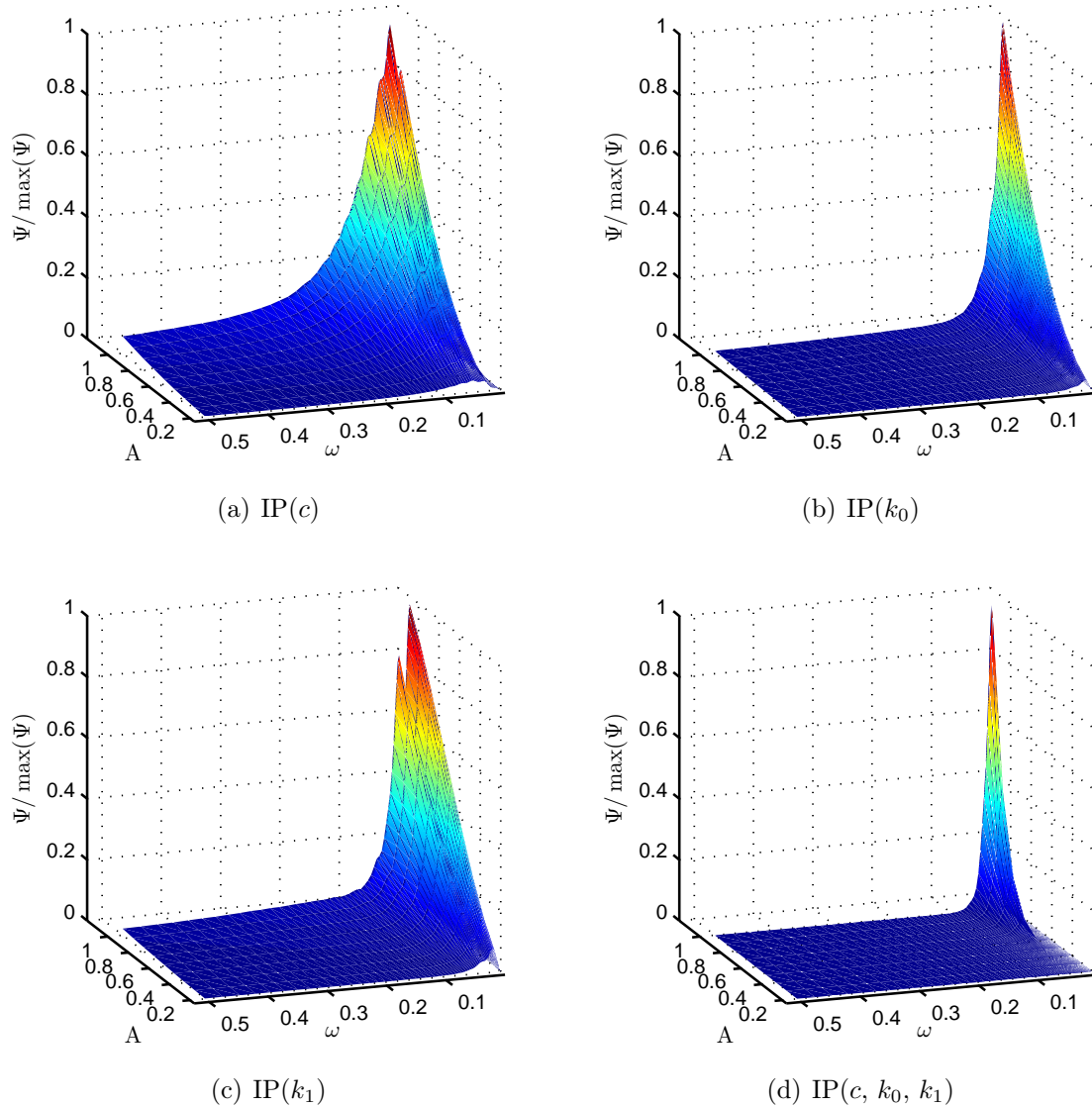


**Figure 3.**  $D$ -optimum criterion  $\Psi$  as a function of  $A$  and  $\omega$  for the 4 different inverse problems ( $N = N^\circ = 1$ ).

### 3. Optimal experiment design for non-linear heat and moisture transfer

In previous section, the concept of optimal experiment design was detailed for an inverse problem of non-linear heat transfer. In this section, the approach goes further by studying optimal experiment design for inverse problems to estimate transport and storage coefficients of heat and moisture transfer.

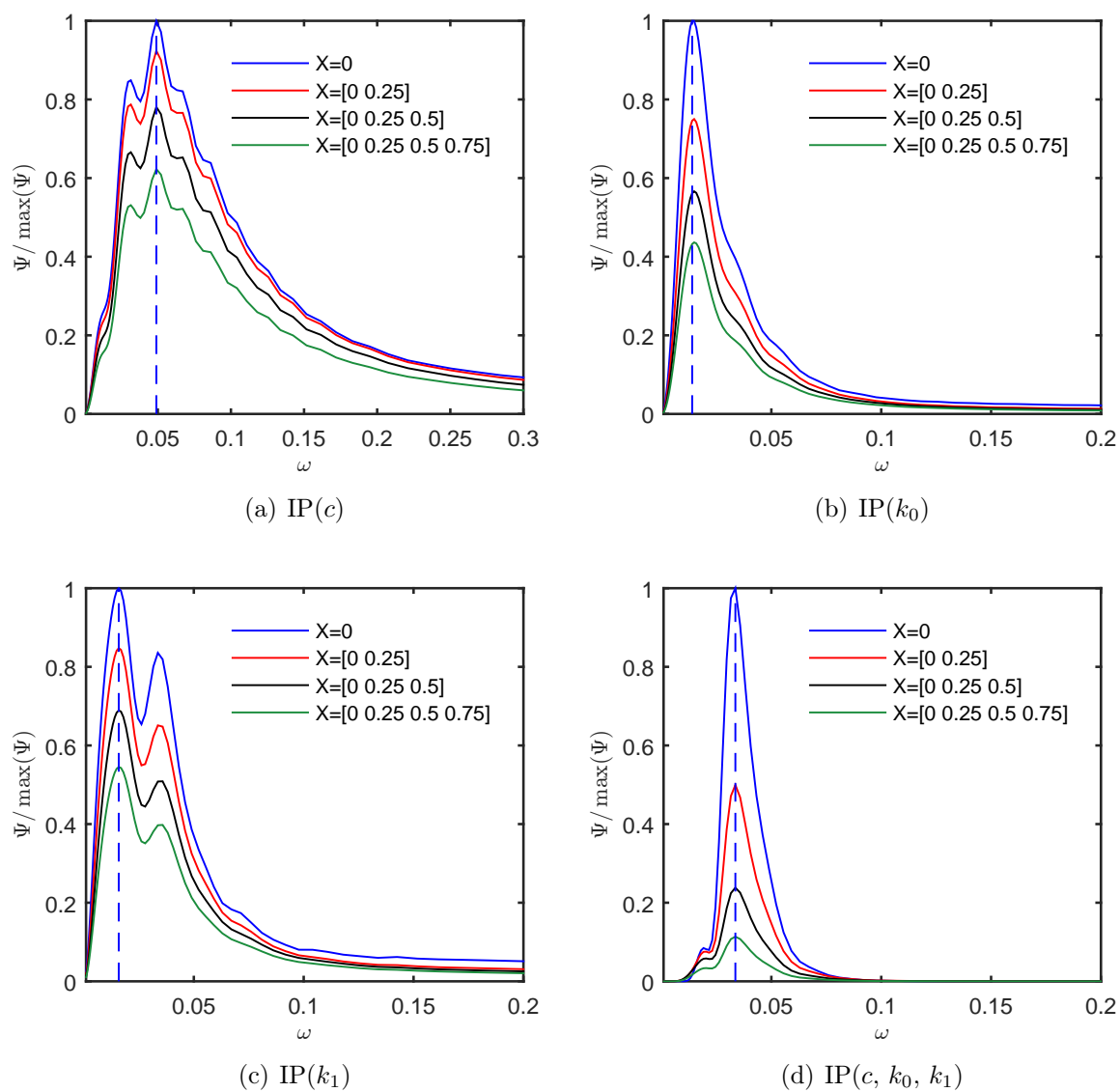


**Figure 4.** *D*-optimum criterion  $\Psi$  as a function of  $N$ ,  $\mathbf{X}$  and  $\omega$  for the 4 different inverse problems ( $A = A^\circ = 1$ ).

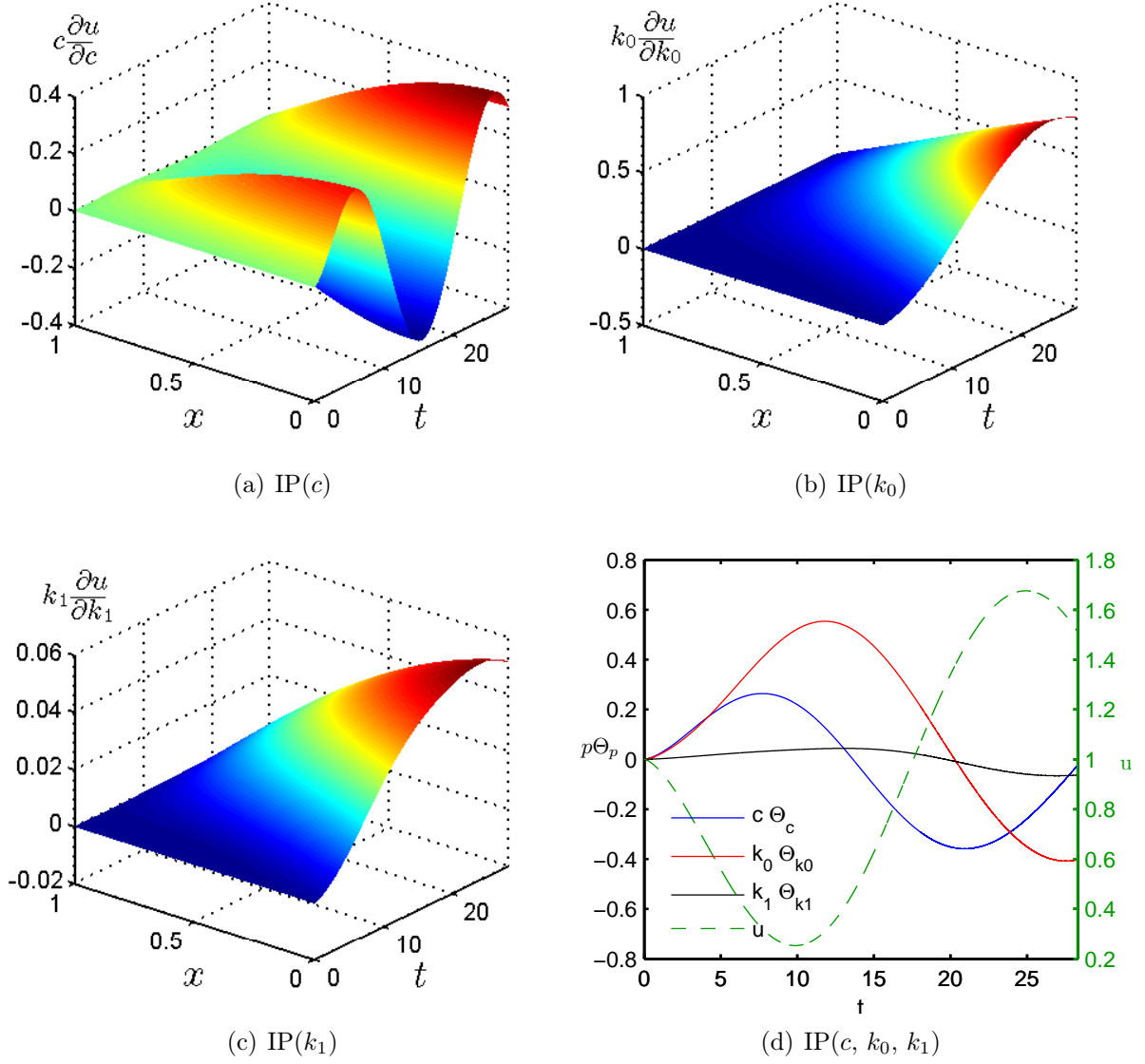


**Figure 5.** Sensitivity coefficient of parameters for the four different inverse problems ( $N = N^\circ = 1$ ).

### 3.1. Physical problem and mathematical formulation

The physical problem concerns a 1–dimensional coupled heat and moisture transfer through a wall based on [3, 17, 18, 21]:

$$c_{10} \frac{\partial T}{\partial t} - \frac{\partial}{\partial x} \left( d_1 \frac{\partial T}{\partial x} \right) - (L_v - c_l T) \frac{\partial}{\partial x} \left( d_2 \frac{\partial P_v}{\partial x} \right) = 0 \quad (3.1a)$$

$$\frac{\partial w}{\partial t} - \frac{\partial}{\partial x} \left( d_2 \frac{\partial P_v}{\partial x} \right) = 0, \quad (3.1b)$$

Inverse problem	max( $\Psi$ )	Optimal experimental design $\pi^\circ$					
		$A^\circ$ [-]	$A^\circ$ [W/m <sup>2</sup> ]	$\frac{1}{\omega^\circ}$ [-]	$\frac{1}{\omega^\circ}$ [h]	$N^\circ$	$X^\circ$
$\mathbf{P} = c$	$1.4 \times 10^{-2}$	1	350	20.4	17.3	1	0
$\mathbf{P} = k_0$	8.6	1	350	71.6	60.6	1	0
$\mathbf{P} = k_1$	3.23	1	350	63.2	53.5	1	0
$\mathbf{P} = (c, k_0, k_1)$	$9.1 \times 10^{-3}$	1	350	29.7	25.2	1	0

**Table 1.** Value of the maximum  $D$ -optimum criterion for each inverse problem.

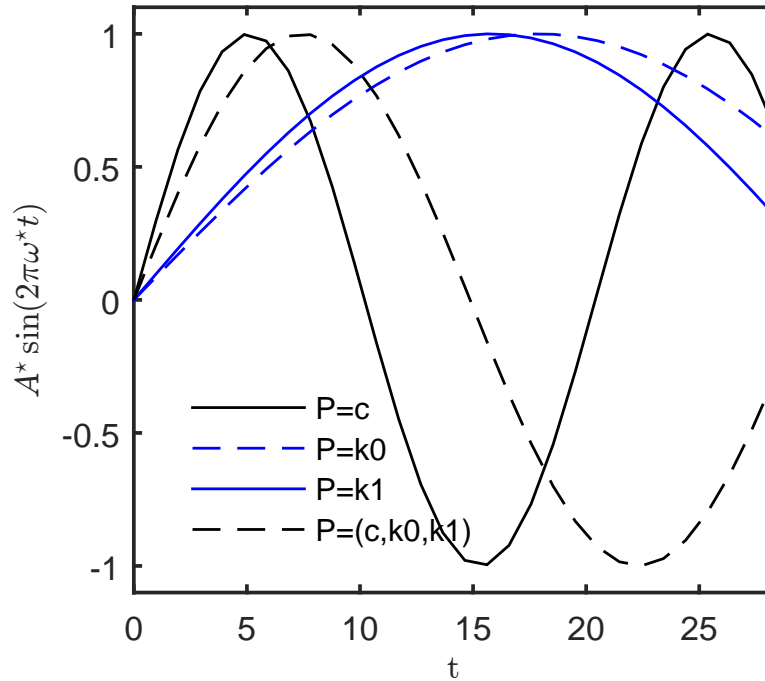


**Figure 6.** Optimal heat flux for the four different inverse problems ( $N = 1$ ).

with  $w$  the water content,  $P_v$  the vapour pressure,  $T$  the temperature,  $d_2$  the vapour permeability,  $c_{10}$  the volumetric thermal capacity,  $d_1$  the thermal conductivity,  $c_l$  the specific heat capacity of water and  $L_v$  the latent heat evaporation. As this study remains

in the hygroscopic range of the material, the liquid transport is not presently taken into account.

The following assumptions are adopted on the properties of the material. The volumetric moisture content is assumed as a first-degree polynomial of the vapour pressure. The vapour permeability and the thermal conductivity are taken as a first-degree polynomial of the volumetric moisture content:

$$\frac{w}{w_0} = c_{20} + \frac{c_{21}}{w_0} P_v \quad (3.2a)$$

$$d_2 = d_{20} + d_{21} \frac{w}{w_0} \quad (3.2b)$$

$$k = d_{10} + d_{11} \frac{w}{w_0}. \quad (3.2c)$$

Based on these equations, the experimental set-up considers a material with uniform initial temperature and vapour pressure. At  $t > 0$ , sinusoidal heat and vapour flux are imposed at boundary  $\Gamma_q = \{x = 0\}$ , while the temperature and vapour pressure are maintained constant at the other boundary  $\Gamma_D = \{x = 1\}$ . The unscaled problem can be formulated as:

$$c_{10}^* \frac{\partial u}{\partial t^*} - \frac{\partial}{\partial x^*} \left( d_1^* \frac{\partial u}{\partial x^*} \right) - (K_{O_1} - K_{O_2}) \text{Lu} \frac{\partial}{\partial x^*} \left( d_2^* \frac{\partial v}{\partial x^*} \right) = 0 \quad x^* \in \Omega, t^* \in ]0, \tau] \quad (3.3a)$$

$$c_{21}^* \frac{\partial v}{\partial t^*} - \text{Lu} \frac{\partial}{\partial x^*} \left( d_2^* \frac{\partial v}{\partial x^*} \right) = 0 \quad x^* \in \Omega, t^* \in ]0, \tau] \quad (3.3b)$$

$$-d_1^* \frac{\partial u}{\partial x^*} = A_1^* \sin(2\pi\omega_1^* t^*) \quad x^* \in \Gamma_q, t^* \in ]0, \tau] \quad (3.3c)$$

$$-d_2^* \frac{\partial v}{\partial x^*} = A_2^* \sin(2\pi\omega_2^* t^*) \quad x^* \in \Gamma_q, t^* \in ]0, \tau] \quad (3.3d)$$

$$u = u_D, \quad v = v_D \quad x^* \in \Gamma_D, t^* \in ]0, \tau] \quad (3.3e)$$

$$u = u_0(x), \quad v = v_0(x) \quad x^* \in \Omega, t^* = 0 \quad (3.3f)$$

$$d_1^* = d_{10}^* + d_{11}^* (c_{20} + c_{21}^* v) \quad (3.3g)$$

$$d_2^* = d_{20}^* + d_{21}^* (c_{20} + c_{21}^* v) \quad (3.3h)$$



with following dimension less ratios:

$$\begin{aligned}
u &= \frac{T}{T_{ref}} & v &= \frac{P_v}{P_{ref}} & u_0 &= \frac{T_0}{T_{ref}} & v_0 &= \frac{P_{v,0}}{P_{ref}} \\
u_D &= \frac{T_D}{T_{ref}} & v_D &= \frac{P_{v,D}}{P_{ref}} & \text{Ko}_1 &= \frac{L_v c_{2,ref}}{c_{1,ref}} \frac{P_{ref}}{T_{ref}} & \text{Ko}_2 &= \frac{c_L c_{2,ref}}{c_{1,ref}} P_{ref} \\
\text{Lu} &= \frac{d_{2,ref} c_{1,ref}}{c_{2,ref} d_{1,ref}} & d_{10}^* &= \frac{d_{10}}{d_{1,ref}} & d_{11}^* &= \frac{d_{11}}{d_{1,ref}} & d_{20}^* &= \frac{d_{20}}{d_{2,ref}} \\
d_{21}^* &= \frac{d_{21}}{d_{2,ref}} & c_{10}^* &= \frac{c_{10}}{c_{1,ref}} & c_{21}^* &= \frac{c_{21}}{c_{2,ref}} & c_{2,ref} &= \frac{w_0}{P_{ref}} \\
A_1^* &= \frac{A_1 L}{d_{1,ref} T_{ref}} & A_2^* &= \frac{A_2 L}{d_{2,ref} P_{ref}} & \omega_1^* &= \omega_1 t_{ref} & \omega_2^* &= \omega_2 t_{ref} \\
t^* &= \frac{t}{t_{ref}} & x^* &= \frac{x}{L} & t_{ref} &= \frac{c_{1,ref} L^2}{d_{1,ref}}
\end{aligned}$$

where  $\text{Ko}$  is the KOSSOVITCH number,  $\text{Lu}$  states for the LUIKOV number,  $L$  is the dimension of the material,  $t_{ref}$  the characteristic time of the problem,  $A$  and  $\omega$  the amplitude and intensity of the heat and vapour flux. Subscripts  $ref$  accounts for a reference value,  $D$  for the DIRICHLET boundary conditions, 0 for the initial condition of the problem, 1 for the heat transfer, 2 for the vapour transfer and superscript  $\star$  for dimensionless parameters.

### 3.2. Optimal experiment design

The OED is sought as a function of the quantity of sensors  $N$  and their locations  $X$  and as a function of the frequencies  $(\omega_1, \omega_2)$  of the heat and vapour flux. According to the results of Section 2.3 and to our numerical investigations, a monotonous increase of the sensitivity of the system were observed with the amplitude  $(A_1, A_2)$  of the flux. Therefore, these parameters were considered as fixed. Thus, the OED aims at finding the measurement plan  $\pi^\circ$  for which the criterion Eqs. (2.5) reaches a maximum value:

$$\pi^\circ = \{N^\circ, \mathbf{X}^\circ, \omega_1^\circ, \omega_2^\circ\} = \arg \max_{\pi} \Psi. \quad (3.4)$$

Parameters  $L_v, c_L$  are physical constants given for the problem. Therefore, considering Eqs. (3.3), a number of 7 parameters can be estimated by the resolution of inverse problems:  $(c_{10}^*, d_{10}^*, d_{11}^*, c_{20}^*, c_{21}^*, d_{20}^*, d_{21}^*)$ . It can focus on the definition of an experiment for the estimation of one single parameter or several parameters. It might be noted that parameters  $(c_{20}^*, c_{21}^*, d_{20}^*, d_{21}^*)$  can be identified by inverse problems considering field  $u, v$  or both  $(u, v)$

as observation. The thermal properties  $(c_{10}^*, d_{10}^*, d_{11}^*)$  can only be estimated using the observation of  $u$ .

All in all, 20 experiments can be defined as:

- (1) 15 for the estimation of a single parameters among  $c_{10}^*, d_{10}^*, d_{11}^*, c_{20}^*, c_{21}^*, d_{20}^*$  or  $d_{21}^*$ ,
- (2) 1 for the estimation of the thermal properties  $(c_{10}^*, d_{10}^*, d_{11}^*)$ ,
- (3) 3 for the estimation of the moisture properties  $(c_{20}^*, c_{21}^*, d_{20}^*, d_{21}^*)$ ,
- (4) 1 for the estimation of the hygrothermal properties (hg)  $(c_{10}^*, d_{10}^*, d_{11}^*, c_{20}^*, c_{21}^*, d_{20}^*, d_{21}^*)$ .

Following notation is adopted:  $\text{IP}(p)[u]$  states for an experiment defined for the estimation of parameter  $p$  using field  $u$  as the observation. The 20 experiments are recalled in Table 2. The same methodology as presented in Section 2 is used. The fifteen sensitivity functions are computed for calculating the criterion (3.4).

### 3.3. Numerical example

The following numerical values are considered for numerical application. The domain  $\Omega$  is defined as  $\Omega = [0, 1]$ , considering the wall thickness of the material as the characteristic length of the problem  $L_r = 0.1$  m. The total time simulation of the experiments is  $\tau = 6 \times 10^3$ , corresponding to a physical simulation of 40 days. The initial and prescribed conditions equal to  $u_D = u_0 = 1$  and  $v_D = v_0 = 0.5$ . The reference temperature and vapour pressure are taken as  $T_{ref} = 293.15$  K and  $P_{v,ref} = 2337$  Pa, respectively. The amplitude of the heat and vapour flux are  $A_1^* = 1.7 \times 10^{-2}$  and  $A_2^* = 1.7$ , equivalent to  $600$  W/m<sup>2</sup> and  $1.2 \times 10^{-7}$  kg/m<sup>3</sup>/s.

The dimension less parameters are:

$$\begin{aligned} \text{Lu} &= 2.5 \times 10^{-4} & \text{Ko}_1 &= 2.1 \times 10^{-1} & \text{Ko}_2 &= 2.5 \times 10^{-2} & d_{10}^* &= 5 \times 10^{-2} & d_{11}^* &= 5 \times 10^{-3} \\ d_{20}^* &= 1 & d_{21}^* &= 0.4 & c_{10}^* &= 1 & c_{20}^* &= 2 & c_{21}^* &= 6 \end{aligned}$$

The properties corresponds to a wood fibre material [3, 17]. They are given in its physical dimension in Appendix A.

The OED is sought as a function of the number of the sensors  $N$ . It varies from  $N = 1$ , located at  $X = [0]$ , to  $N = 3$ , located at  $X = [0 \ 0.2 \ 0.4]$ . The OED is also investigated as a function of the frequencies  $(\omega_1^*, \omega_2^*)$  of the flux. For each frequency, 20 values are taken in the interval  $[1 \times 10^{-5}; 1.5 \times 10^{-3}]$ . The minimal and maximal values correspond to a flux having a physical period of 495 days and 3.3 days, respectively.

As mentioned in Section 2.2, the computation of the solution of the optimal experiment plan is done by successive iterations for the whole grid of the measurement plan  $\pi = \{N, X, \omega_1, \omega_2\}$ .

#### 3.3.1 Estimation of one single parameter

In the current section, the OED is sought for inverse problems to estimate one single parameter among  $c_{10}^*, d_{10}^*, d_{11}^*, c_{20}^*, c_{21}^*, d_{20}^*$  or  $d_{21}^*$ . The results of the ODE are given in Table 2 for the physical values and in Figure 9(b) for the dimensionless values.

The criterion  $\Psi$  varies actively with the frequencies  $(\omega_1^*, \omega_2^*)$  for inverse problem of parameter  $c_{10}^*$ , as shown in Figure 7(a). The ODE is reached for a period for the heat and vapour flux of 27.2 days.

On the other hand, Figures 7(b) and 7(c) illustrate that the criterion varies mostly with the frequency  $\omega_1^*$  for inverse problem of parameter  $d_{10}^*$  and  $d_{11}^*$ . The ODE is reached for a period for the heat of 78.1 days. Furthermore, the magnitude of  $\Psi$  is really higher than zero, ensuring a good conditioning to solve inverse problems. As observed in previous section concerning non linear heat transfer (Section 2.3), the period of the heat flux is smaller for the ODE of the thermal capacity than for the thermal conductivity.

In Figure 10, the sensitivity functions of parameters  $d_{10}^*$  is given for experimental conditions  $\pi$  where  $\Psi$  reaches its minimal value and for the ODE conditions. In Figure 10(a), the magnitude of the sensitivity function is really small (at an order of  $10 \times 10^{-3}$ ) explaining why the criterion  $\Psi$  is minimum for these conditions. In Figure 10(b), it can be noticed the sensitivity function is maximal on the boundary  $\Gamma_q = \{x = 0\}$ . It emphasizes why the criterion  $\Psi$  is maximal for a single sensor settled at this boundary.

For inverse problems of the vapour properties,  $c_{20}^*$ ,  $c_{21}^*$ ,  $d_{20}^*$  or  $d_{21}^*$ , the ODE is not very sensitive to the frequency of the heat flux as reported in Figures 7(d), 7(e), 7(f) and 8(a). It can be noted that the criterion  $\Psi$  is higher when dealing with inverse problem considering fields  $(u, v)$  as observations. The computational algorithm to solve the inverse problem is better conditioned. The period of the ODE vapour flux is 9.5 and 12.3 days for inverse problems of  $d_{20}^*$  and  $c_{21}^*$ . Inverse problems of  $d_{21}^*$  and  $c_{20}^*$  have the same period of the ODE vapour flux (27.2 days).

It might be recalled that this analysis has been done for a fixed and constant error measurement, equals for the temperature and vapour pressure sensors. Indeed, this hypothesis can be revisited in practical applications. Furthermore, if only one field is available to estimate the vapour properties  $(u$  or  $v)$ , it is required to use the field  $v$  as observation and prioritize the accuracy for those sensors. The criterion  $\Phi$  and the sensitivity is highest for the field  $v$  as shown in Figures 11(a) and 11(b).

For all inverse problems, a single sensor located at  $x = 0$  is sufficient for the ODE as shown in Table 2. The surface receiving the heat and vapour flux is where the sensitivity of the parameters is the higher as illustrated in Figures 11(a) and 11(b) for the parameter  $c_{21}$ .

### 3.3.2 Estimation of several parameters

The optimal experiment design is now sought for inverse problems to estimate several parameters: the thermo-physical properties  $(c_{10}^*, d_{10}^*, d_{11}^*)$ , the moisture properties  $(c_{20}^*, c_{21}^*, d_{20}^*, d_{21}^*)$  and the hygrothermal (hg) coefficients  $(c_{10}^*, d_{10}^*, d_{11}^*, c_{20}^*, c_{21}^*, d_{20}^*, d_{21}^*)$ . Five inverse problems are considered for the estimation of these parameters as reported in Table 2.

For the estimation of the hygrothermal properties, Figure 8(b) shows that the criterion  $\Psi$  varies mostly with frequency  $\omega_1^*$ . The criterion is very close to zero (an order of  $\mathcal{O}(10^{-9})$ ). The computational algorithm for the solution of the inverse problem might be ill conditioned.

The results of the inverse problem might not be accurate. A way to circumvent the problem is to increase the precision of the sensors and the amplitude of the heat and vapour fluxes.

According to Table 2, the vapour properties might be estimated using both fields  $(u, v)$ . If it is not possible, the field  $v$  would give a more accurate estimation than field  $u$ . The criterion varies mostly with the frequency  $\omega_1^*$  of the heat flux, Figure 8(c). The ODE is reached for a period of 35.4 and 16 days for the heat and vapour fluxes respectively.

For the thermal properties, the criterion varies with both heat and vapour flux frequencies, as reported in Figure 8(d). A period of 16 days for both fluxes yields the ODE.

The variation of the criterion with the quantity of sensors is given in Figure 12. A single sensor is sufficient for the ODE of all inverse problems except for the estimation of the hygrothermal properties. In such case, the ODE is achieved for 2 sensors, located at  $x = 0$  and  $x = 0.2$  m.

## 4. Conclusion

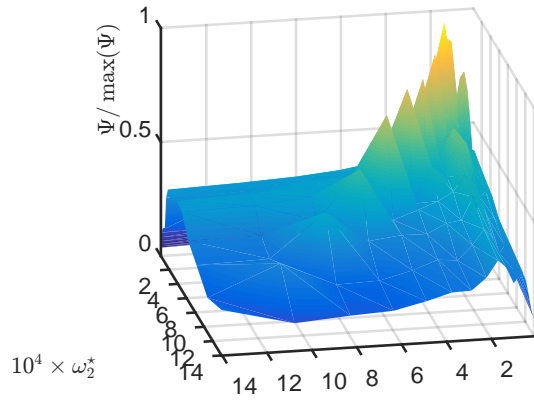
In the context of estimating material properties, using in-site measurements of wall in test cells or real buildings combined with identification methods, this study explored the concept of optimal experiment design (OED). It aimed at searching the best experimental conditions in terms of quantity and location of sensors and flux imposed to the material. These conditions ensure to provide the best accuracy of the identification method and thus the estimated parameter. The search of the OED was done using the Fisher information matrix, quantifying the amount of information contained in the observed field.

Two cases were illustrated. The first one deals with an inverse problem of non-linear heat transfer to estimate the thermal properties (storage and transport coefficients). The experiment considers a uniform initial temperature. The material is submitted to a fixed prescribed temperature on one side and a sinusoidal flux on the other, for 24 hours. The ODE yields in using one single temperature sensor located at the surface receiving the flux. The flux should have an intensity of  $350 \text{ W/m}^2$  and periods of 17.3 h, 60.6 h, 53.5 h and 25.2 h for inverse problems to estimate, respectively, the thermal capacity, the thermal conductivity, the temperature dependent conductivity and all parameters.

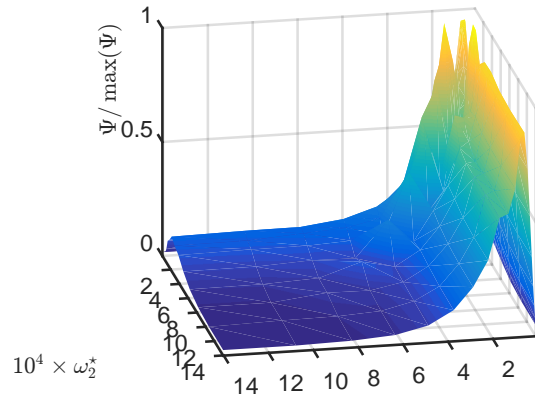
The second application concerned experiments for inverse problems of non-linear heat and moisture transfer to estimate the hygrothermal properties of the material. The experiment is similar to the first case study. Uniform initial distribution of temperature and vapour pressure were considered. It is submitted to harmonic heat and vapour fluxes at one side and prescribed temperature and vapour pressure values at the other. The experiment is done for a period of 40 days. The achievement of the ODE was explored for different inverse problems, aiming at estimating one or several parameters. As the equation considered are weakly coupled, the thermal properties can only be determined using the temperature. The accuracy of the identification method does not depend on the vapour flux. For the vapour properties, results have shown that the estimation will be more accurate using the temperature and vapour pressure as observations. Furthermore, the accuracy actively depends on the period of the vapour flux. Single sensor has to be located at the side where

<i>Inverse problem</i>	$\max \{ \Psi \}$	<i>Optimal experimental design <math>\pi^*</math></i>		
		$\frac{2\pi}{\omega_1^\circ}$ (days)	$\frac{2\pi}{\omega_2^\circ}$ (days)	$N^\circ$
IP( $c_{10}$ )[ $u$ ]	6.03	27.2	27.2	1
IP( $d_{10}$ )[ $u$ ]	288	78.1	20.9	1
IP( $d_{11}$ )[ $u$ ]	181	78.1	101.7	1
IP( $d_{20}$ )[ $u$ ]	0.53	7.3	7.3	1
IP( $d_{20}$ )[ $v$ ]	0.99	60	9.5	1
IP( $d_{20}$ )[ $u, v$ ]	1.53	9.5	9.5	1
IP( $d_{21}$ )[ $u$ ]	133	78.1	27.2	1
IP( $d_{21}$ )[ $v$ ]	140	9.5	27.2	1
IP( $d_{21}$ )[ $u, v$ ]	276	78.1	27.2	1
IP( $c_{20}$ )[ $u$ ]	0.02	20.9	20.9	1
IP( $c_{20}$ )[ $v$ ]	0.03	9.5	27.2	1
IP( $c_{20}$ )[ $u, v$ ]	0.05	27.2	27.2	1
IP( $c_{21}$ )[ $u$ ]	0.004	35.4	20.9	1
IP( $c_{21}$ )[ $v$ ]	0.014	78.1	12.3	1
IP( $c_{21}$ )[ $u, v$ ]	0.017	78.1	12.3	1
IP( $hg$ )[ $u, v$ ]	$4.5 \times 10^{-9}$	27.2	12.3	2
IP( $c_{20}, c_{21}, d_{20}, d_{21}$ )[ $u$ ]	0.001	60.0	20.9	1
IP( $c_{20}, c_{21}, d_{20}, d_{21}$ )[ $v$ ]	0.15	12.3	27.2	1
IP( $c_{20}, c_{21}, d_{20}, d_{21}$ )[ $u, v$ ]	0.2	35.4	16	1
IP( $c_{10}, d_{10}, d_{11}$ )[ $u$ ]	137	16	16	1

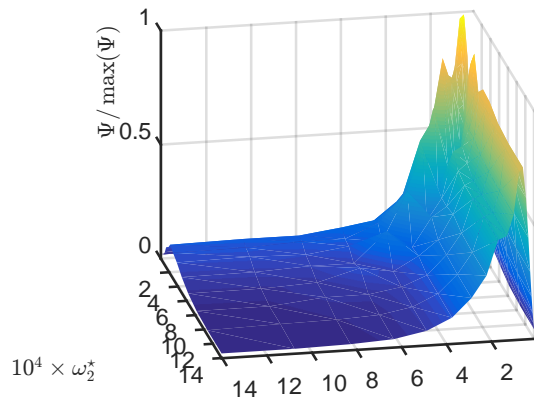
**Table 2.** Value of the maximum D-optimum criterion for each inverse problem.



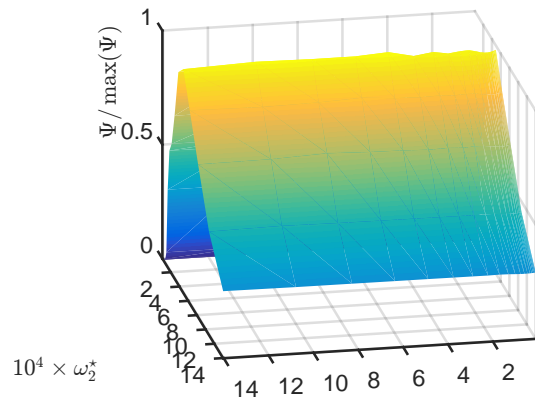
$10^4 \times \omega_1^*$   
(a)  $\text{IP}(c_{10})[u], N = 1$



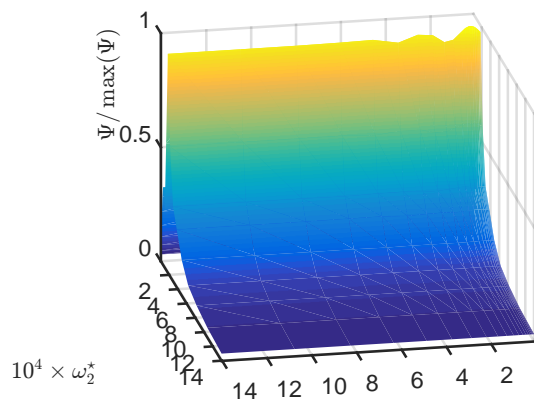
$10^4 \times \omega_1^*$   
(b)  $\text{IP}(d_{10})[u], N = 1$



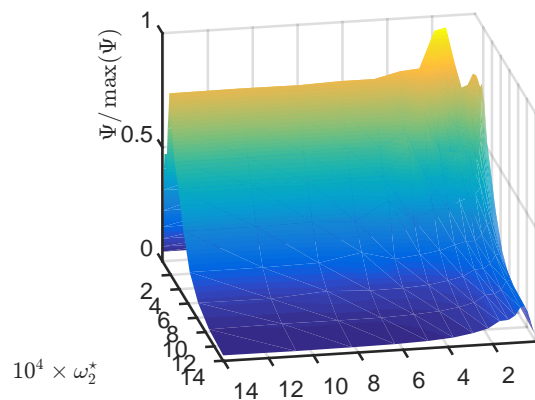
$10^4 \times \omega_1^*$   
(c)  $\text{IP}(d_{11})[u], N = 1$



$10^4 \times \omega_1^*$   
(d)  $\text{IP}(d_{20})[u,v], N = 1$



$10^4 \times \omega_1^*$   
(e)  $\text{IP}(d_{21})[u,v], N = 1$



$10^4 \times \omega_1^*$   
(f)  $\text{IP}(c_{20})[u,v], N = 1$

**Figure 7.**  $D$ -optimum criterion  $\Psi$  as a function of the frequencies  $(\omega_1, \omega_2)$ .

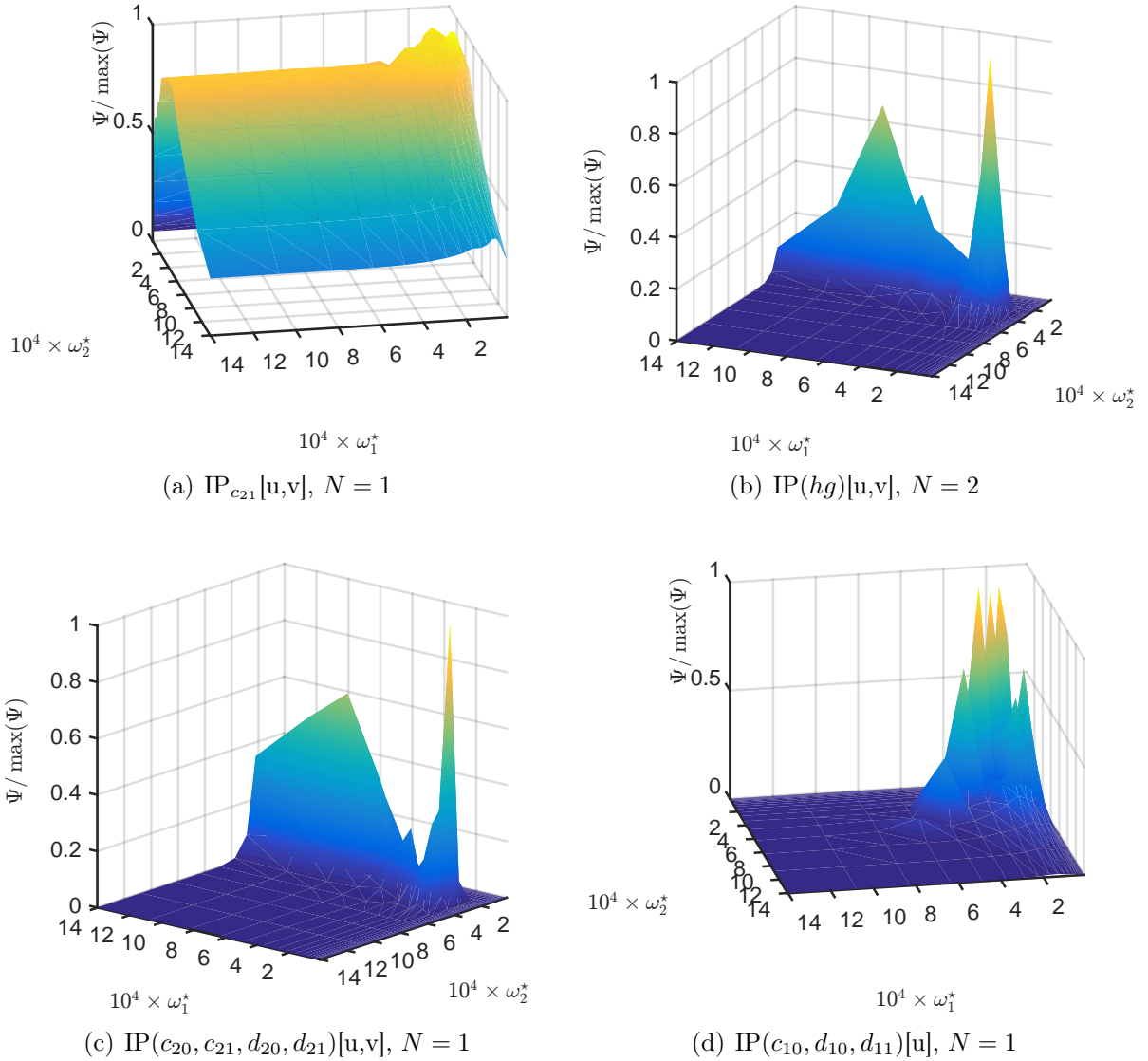


**Figure 8.** *D*-optimum criterion  $\Psi$  as a function of the frequencies  $(\omega_1, \omega_2)$ .

the flux is imposed. For inverse problems to estimate all the hygrothermal properties, two sensors improve the accuracy accuracy.

This contribution explored the concept of optimal experiment design for application in building physics for estimating the hygrothermal properties of materials. The methodology of searching the ODE is important before starting any experiment aiming at solving estimation parameter problems. With a priori values of the unknown parameters, the sensitivity functions and the optimum criterion can be computed. Results allow choosing by means of deterministic approach the conditions of the experiments. A good design of experiments avoids installing unnecessary sensors. In the case of coupled phenomena, as

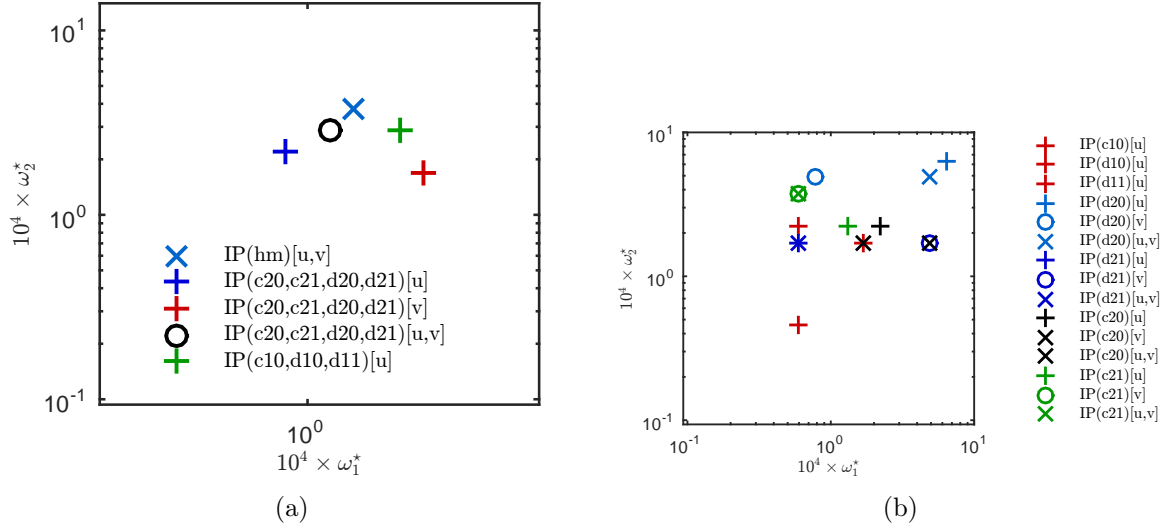


**Figure 9.** Frequencies  $(\omega_1^{*\circ}, \omega_2^{*\circ})$  of the ODE.

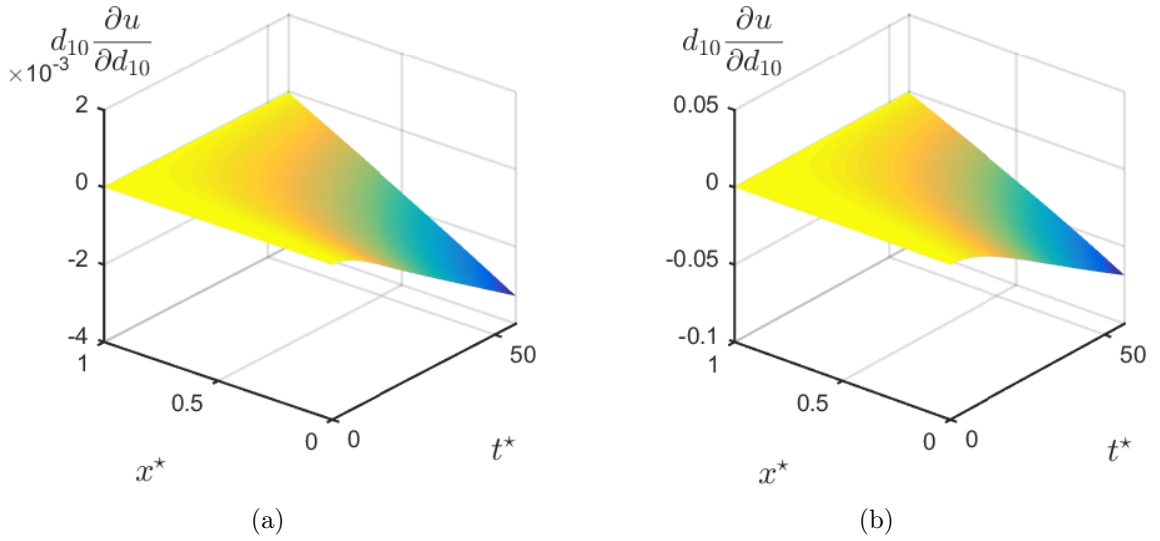


**Figure 10.** Sensitivity coefficient of parameter  $k_0$  for experimental conditions  $\pi$  where  $\Psi$  reaches its minimal value (a)  $(\frac{2\pi}{\omega_1} = 3.3$  days,  $\frac{2\pi}{\omega_2} = 495$  days,  $N = 3$ ) and for the ODE conditions (b)  $(\frac{2\pi}{\omega_1^\circ} = 78.1$  days,  $\frac{2\pi}{\omega_2^\circ} = 20.9$  days,  $N^\circ = 1$ ).

heat and moisture transfer, considering sensor accuracies, it enables to choose and select the field that must be monitored. It also improves the accuracy of the solution of the estimation problems.

Future work will have to explore the application of the OED to real experimental data.



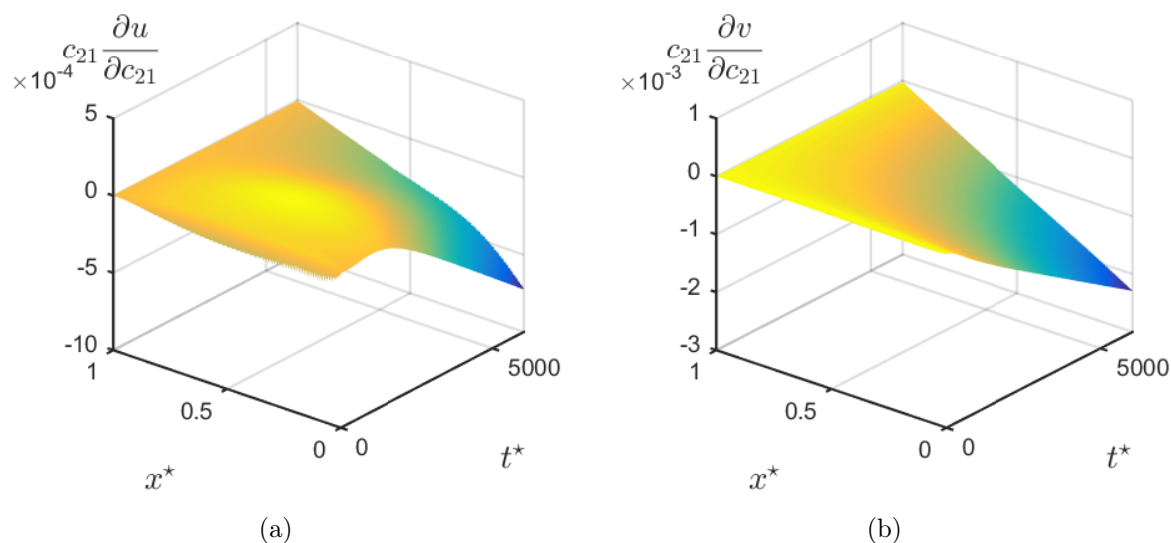


**Figure 11.** Sensitivity coefficient of parameter  $c_{21}$  for the ODE conditions of  $IP(c_{21})[u, v]$ .

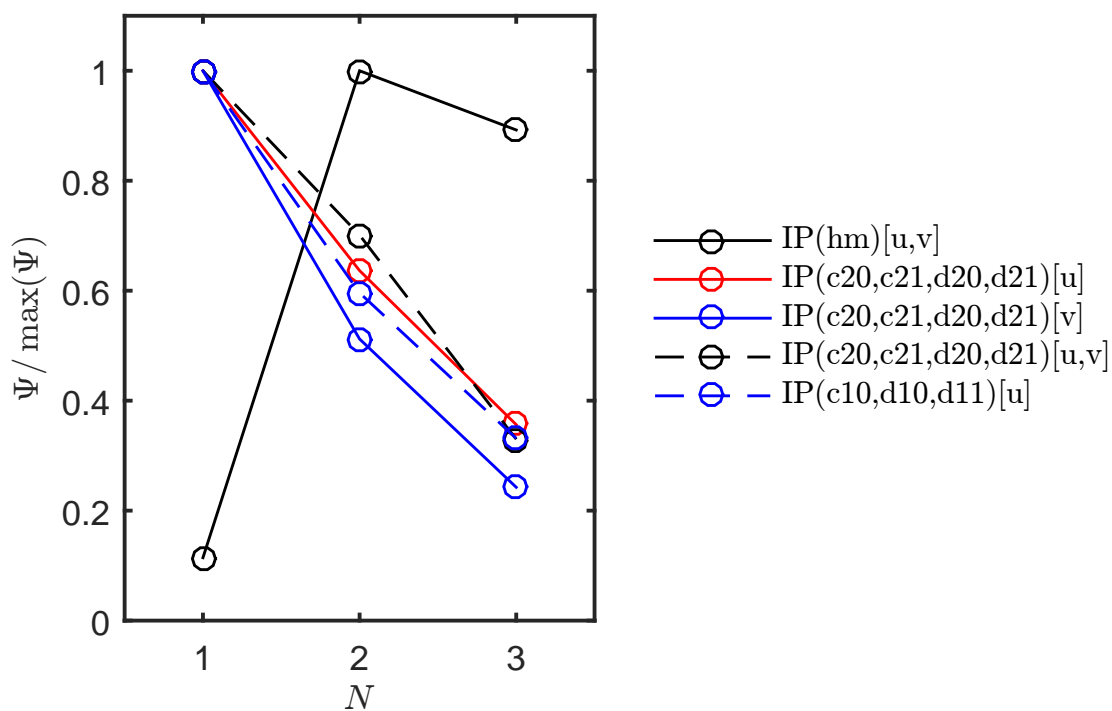


**Figure 12.**  $D$ -optimum criterion  $\Psi$  as a function of the quantity of sensors  $N$ .

<i>Property</i>	<i>Value</i>
$d_{10}$ [W/m/K]	0.5
$d_{11}$ [W/m/K/Pa]	0.05
$d_{20}$ [s]	$2.5 \times 10^{-11}$
$d_{21}$ [s/Pa]	$1 \times 10^{-11}$
$c_{11}$ [J/m <sup>3</sup> /K]	$4 \times 10^5$
$c_{20}$ [-]	2
$c_{21}$ [s <sup>2</sup> /m <sup>2</sup> ]	$2.5 \times 10^{-2}$
<i>Physical constant</i>	<i>Value</i>
$L_v$ [J/kg]	$2.5 \times 10^6$
$c_L$ [J/kg]	1000

**Table 3.** *Hygrothermal properties of the material.*

## Acknowledgments

The Authors acknowledge the Brazilian Agencies CAPES of the Ministry of Education and the CNPQ of the Ministry of Science, Technology and Innovation for the financial support. D. DUTYKH also acknowledges the hospitality of PUCPR during his visit in April 2016.

## A. Hygrothermal properties

The hygrothermal properties of the material used in Section 3.3 are given in Table 3.

## References

- [1] E. A. Artyukhin and S. A. Budnik. Optimal planning of measurements in numerical experiment determination of the characteristics of a heat flux. *Journal of Engineering Physics*, 49(6):1453–1458, dec 1985. 4, 6, 7
- [2] J. V. Beck and K. J. Arnold. *Parameter Estimation in Engineering and Science*. John Wiley & Sons, Inc., New York, 1977. 7
- [3] J. Berger, M. Chhay, S. Guernouti, and M. Woloszyn. Proper generalized decomposition for solving coupled heat and moisture transfer. *Journal of Building Performance Simulation*, 8(5):295–311, sep 2015. 12, 16
- [4] R. Cantin, J. Burgholzer, G. Guarracino, B. Moujalled, S. Tamelikecht, and B. Royet. Field assessment of thermal behaviour of historical dwellings in France. *Building and Environment*,

- 45(2):473–484, feb 2010. [3](#)
- [5] T. Colinart, D. Lelievre, and P. Glouannec. Experimental and numerical analysis of the transient hygrothermal behavior of multilayered hemp concrete wall. *Energy and Buildings*, 112:1–11, jan 2016. [3](#)
- [6] T. Z. Desta, J. Langmans, and S. Roels. Experimental data set for validation of heat, air and moisture transport models of building envelopes. *Building and Environment*, 46(5):1038–1046, may 2011.
- [7] C. James, C. J. Simonson, P. Talukdar, and S. Roels. Numerical and experimental data set for benchmarking hygroscopic buffering models. *Int. J. Heat Mass Transfer*, 53(19-20):3638–3654, sep 2010.
- [8] T. Kalamees and J. Vinha. Hygrothermal calculations and laboratory tests on timber-framed wall structures. *Building and Environment*, 38(5):689–697, may 2003. [3](#)
- [9] M. Karalashvili, W. Marquardt, and A. Mhamdi. Optimal experimental design for identification of transport coefficient models in convection-diffusion equations. *Computers & Chemical Engineering*, 80:101–113, sep 2015. [3](#), [4](#), [7](#)
- [10] M. Labat, M. Woloszyn, G. Garnier, and J. J. Roux. Dynamic coupling between vapour and heat transfer in wall assemblies: Analysis of measurements achieved under real climate. *Building and Environment*, 87:129–141, may 2015. [3](#)
- [11] D. Lelievre, T. Colinart, and P. Glouannec. Hygrothermal behavior of bio-based building materials including hysteresis effects: Experimental and numerical analyses. *Energy and Buildings*, 84:617–627, dec 2014. [3](#)
- [12] T. Metzger, S. Didierjean, and D. Maillet. Optimal experimental estimation of thermal dispersion coefficients in porous media. *Int. J. Heat Mass Transfer*, 47(14-16):3341–3353, jul 2004. [4](#)
- [13] A. Nassiopoulos and F. Bourquin. On-Site Building Walls Characterization. *Numerical Heat Transfer, Part A: Applications*, 63(3):179–200, jan 2013. [3](#)
- [14] A. V. Nenarokomov and D. V. Titov. Optimal experiment design to estimate the radiative properties of materials. *Journal of Quantitative Spectroscopy and Radiative Transfer*, 93(1-3):313–323, jun 2005. [4](#), [6](#), [7](#)
- [15] M. N. Ozisik and H. R. B. Orlande. *Inverse Heat Transfer: Fundamentals and Applications*. CRC Press, New York, 2000. [6](#)
- [16] H. Rafidiarison, R. Rémond, and E. Mougel. Dataset for validating 1-D heat and mass transfer models within building walls with hygroscopic materials. *Building and Environment*, 89:356–368, jul 2015. [3](#)
- [17] S. Rouchier, M. Woloszyn, Y. Kedowide, and T. Béjat. Identification of the hygrothermal properties of a building envelope material by the covariance matrix adaptation evolution strategy. *Journal of Building Performance Simulation*, 9(1):101–114, jan 2016. [3](#), [12](#), [16](#)
- [18] H.-J. Steeman, M. Van Belleghem, A. Janssens, and M. De Paepe. Coupled simulation of heat and moisture transport in air and porous materials for the assessment of moisture related damage. *Building and Environment*, 44(10):2176–2184, oct 2009. [12](#)
- [19] E. Stéphan, R. Cantin, A. Caucheteux, S. Tasca-Guernouti, and P. Michel. Experimental assessment of thermal inertia in insulated and non-insulated old limestone buildings. *Building and Environment*, 80:241–248, oct 2014. [3](#)
- [20] P. Talukdar, S. O. Olutmayin, O. F. Osanyintola, and C. J. Simonson. An experimental data set for benchmarking 1-D, transient heat and moisture transfer models of hygroscopic building materials. Part I: Experimental facility and material property data. *Int. J. Heat*

- Mass Transfer*, 50(23-24):4527–4539, nov 2007. 3
- [21] F. Tariku, K. Kumaran, and P. Fazio. Transient model for coupled heat, air and moisture transfer through multilayered porous media. *Int. J. Heat Mass Transfer*, 53(15-16):3035–3044, jul 2010. 12
- [22] S. Tasca-Guernouti, B. Flament, L. Bourru, J. Burgholzer, A. Kindinis, R. Cantin, B. Moujalled, G. Guarracino, and T. Marchal. Experimental Method to determine Thermal Conductivity, and Capacity Values in Traditional Buildings. In *VI Mediterranean Congress of Climatization*, Madrid, Spain, 2011. 3
- [23] D. Ucinski. *Optimal Measurement Methods for Distributed Parameter System Identification*. 2004. 3, 7
- [24] A. Zaknounge, P. Glouannec, and P. Salagnac. Estimation of moisture transport coefficients in porous materials using experimental drying kinetics. *Heat and Mass Transfer*, 48(2):205–215, feb 2012. 3

THERMAL SYSTEMS LABORATORY, MECHANICAL ENGINEERING GRADUATE PROGRAM, PONTIFICAL CATHOLIC UNIVERSITY OF PARANÁ, RUA IMACULADA CONCEIÇÃO, 1155, CEP: 80215-901, CURITIBA – PARANÁ, BRAZIL

*E-mail address:* Julien.Berger@pucpr.edu.br

*URL:* [https://www.researchgate.net/profile/Julien\\_Berger3/](https://www.researchgate.net/profile/Julien_Berger3/)

LAMA, UMR 5127 CNRS, UNIVERSITÉ SAVOIE MONT BLANC, CAMPUS SCIENTIFIQUE, 73376 LE BOURGET-DU-LAC CEDEX, FRANCE

*E-mail address:* Denys.Dutykh@univ-savoie.fr

*URL:* <http://www.denys-dutykh.com/>

THERMAL SYSTEMS LABORATORY, MECHANICAL ENGINEERING GRADUATE PROGRAM, PONTIFICAL CATHOLIC UNIVERSITY OF PARANÁ, RUA IMACULADA CONCEIÇÃO, 1155, CEP: 80215-901, CURITIBA – PARANÁ, BRAZIL

*E-mail address:* Nathan.Mendes@pucpr.edu.br

*URL:* [https://www.researchgate.net/profile/Nathan\\_Mendes/](https://www.researchgate.net/profile/Nathan_Mendes/)